Computing Compressible Two-Component Flow Systems Using Diffuse Interface Method

A. Ballil, S. A. Jolgam, A. F. Nowakowski and F. C. G. A. Nicolleau

Abstract Numerical simulation of compressible two-component flows that consider different materials and physical properties is conducted. An explicit finite volume numerical framework based on an extended second order Godunov approach is developed and implemented to solve an Eulerian type mathematical model. This model consists of five partial differential equations in one space dimension and it is known as the transport reduced model. A fixed Eulerian mesh is considered and the hyperbolic problem is tackled using a robust and efficient HLL Riemann solver. The performance of the numerical solver is verified against a comprehensive suite of numerical and experimental case studies in multi-dimensional space. Computing the evolution of interfaces between two immiscible fluids is considered as a major challenge for the present model and the numerical technique. The achieved numerical results demonstrate a very good agreement with all reference data.

Keywords Compressible multi-component flows · Godunov approach · HLL Riemann solver · Interface evolution · Shock wave · Shock bubble interaction

A. Ballil (✉) · S. A. Jolgam · A. F. Nowakowski · F. C. G. A. Nicolleau
Sheffield Fluid Mechanics Group, Mechanical Engineering Department,
University of Sheffield, Sheffield S1 3JD, UK
e-mail: a.ballil@Sheffield.ac.uk

S. A. Jolgam
e-mail: mep08saj@Sheffield.ac.uk

A. F. Nowakowski
e-mail: a.f.nowakowski@Sheffield.ac.uk

F. C. G. A. Nicolleau
e-mail: f.nicoleau@Sheffield.ac.uk

G.-C. Yang et al. (eds.), *IAENG Transactions on Engineering Technologies*,
Lecture Notes in Electrical Engineering 229, DOI: 10.1007/978-94-007-6190-2_11,

1 Introduction

The numerical simulation of the creation and evolution of interfaces in compressible multi-component flows is a challenging research issue. Multi-component flows occur in several industries and engineering operations such as power generation, separation and mixing processes and the inertial confinement fusion [1]. Computation of this type of flow is complicated and causes some difficulties in various engineering applications such as safety of nuclear reactors [2]. Compressible multi-component flows can be represented numerically by two main approaches. These are: Sharp Interface Method (SIM) and Diffuse Interface Method (DIM). The main characteristic of the DIM is that it allows numerical diffusion at the interface. The DIM corresponds to different mathematical models and various successful numerical approaches: for instance, a seven equation model with two velocities and two pressures developed in [3]; a five equation model proposed in [4] known as the transport reduced model; a similar five equation model was derived from the generic seven equation model in [5] and other two reduced models derived in [6]. This paper introduces the development of the numerical algorithm which utilizes the mathematical model for compressible two-component flows first presented in [4]. The performance of the reduced mathematical models was investigated in [5] and [7] using classical benchmark test problems and Roe type solver. The performance of a numerical framework that has been developed based on this model using HLL and HLLC Riemann solvers has been examined in [8].

In this work an extension of our work in [8] has been made. Computation of compressible two-component flows with different materials and tracking the evolution of the interface between two immiscible fluids is the main aim of the present work. An extended numerical approach has been developed for tracking the interface evolution. The mathematical equations and the main procedures of the numerical framework have been stated for two-dimensional flow systems. The results have been re-demonstrated in the two dimensional case studies with more details. We also have extended the investigation of the performance of the developed numerical algorithm by computing a numerically challenging shock-bubble interaction problem and compare the results with available experimental data. Shock-bubble interaction is a well known multi-component flow phenomenon. It is common in many engineering applications; for example, during supersonic combustion in ramjet engine.

In the framework of multi-component flows with interface evolution and shock bubble interaction many interesting experiments have been carried out. For example, experiments to observe the interaction between a plane shock wave and various gas bubbles were presented in [9]. The deformation of a spherical bubble impacted by a plane shock wave via a multiple exposure shadow-graph diagnostic was examined in [10]. Quantitative comparisons between the experimental data and numerical results of shock-bubble interactions were made in [11]. On the other hand, many numerical simulations of compressible multi-component flows that consider the evolution of the interface have been made. For instance, a numerical method based on upwind schemes was introduced and applied to several two phase flows test problems in [12].

The interaction of the shock wave with various Mach numbers with a cylindrical bubble was investigated numerically in [13]. An interface interaction method for compressible multifluids was developed in [14]. An efficient method to simulate and track fluid interfaces called A front-tracking method was presented in [15]. A new finite-volume interface capturing method was introduced for simulation of multi-component compressible flows with high density ratios and strong shocks in [16].

This paper is organized as follows: The governing equations of the two component flow model are reviewed. The major steps of the numerical method are then described with the HLL Riemann solver. The obtained results are presented. Finally, the conclusion is made.

2 The Mathematical Equations

2.1 The Transport Reduced Model

The two-component flow model that has been considered in this work consists of six equations in 2d flows. It is structured as: Two continuity equations, two mixture momentum equations, a mixture energy equations augmented by a volume fraction equation.

Without mass and heat transfer the model can be written as follows:

$$\begin{aligned}
&\tfrac{\partial \alpha_1}{\partial t} + u\tfrac{\partial \alpha_1}{\partial x} + v\tfrac{\partial \alpha_1}{\partial y} = 0,\\
&\tfrac{\partial \alpha_1\rho_1}{\partial t} + \tfrac{\partial \alpha_1\rho_1 u}{\partial x} + \tfrac{\partial \alpha_1\rho_1 v}{\partial y} = 0,\\
&\tfrac{\partial \alpha_2\rho_2}{\partial t} + \tfrac{\partial \alpha_2\rho_2 u}{\partial x} + \tfrac{\partial \alpha_2\rho_2 v}{\partial y} = 0,\\
&\tfrac{\partial \rho u}{\partial t} + \tfrac{\partial (\rho u^2+P)}{\partial x} + \tfrac{\partial \rho uv}{\partial y} = 0,\\
&\tfrac{\partial \rho v}{\partial t} + \tfrac{\partial \rho uv}{\partial x} + \tfrac{\partial (\rho v^2+P)}{\partial y} = 0,\\
&\tfrac{\partial \rho E}{\partial t} + \tfrac{\partial (u(\rho E+P))}{\partial x} + \tfrac{\partial (v(\rho E+P))}{\partial y} = 0\,.
\end{aligned} \tag{1}$$

The notations are conventional: α_k and ρ_k characterize the volume fraction and the density of the kth component of the flow, ρ, u, v, P and E represent the mixture density, the mixture velocity component in $x-$direction, the mixture velocity component in $y-$direction, the mixture pressure and the mixture total energy respectively.

The mixture variables can be defined as:

$$\begin{aligned}
\rho &= \alpha_1\rho_1 + \alpha_2\rho_2\\
u &= (\alpha_1\rho_1 u_1 + \alpha_2\rho_2 u_2)/\rho\\
v &= (\alpha_1\rho_1 v_1 + \alpha_2\rho_2 v_2)/\rho\\
P &= \alpha_1 P_1 + \alpha_2 P_2\\
E &= (\alpha_1\rho_1 E_1 + \alpha_2\rho_2 E_2)/\rho.
\end{aligned}$$

2.2 Equation of State (EOS)

In the present work, the isobaric closure is used with stiffened equation of state to close the model. The mixture stiffened (EOS) can be cast in the following form:

$$P = (\gamma - 1)\ \rho e - \gamma \pi, \tag{2}$$

where e is the internal energy, γ is the heat capacity ratio and π is the pressure constant.

The mixture equation of state parameters γ and π can be written as:

$$\frac{1}{\gamma - 1} = \sum_k \frac{\alpha_k}{\gamma_k - 1} \quad and \quad \gamma\pi = \frac{\sum_k \frac{\alpha_k \gamma_k \pi_k}{\gamma_k - 1}}{\sum_k \frac{\alpha_k}{\gamma_k - 1}},$$

where k refers to the kth component of the flow.

The internal energy can be expressed in terms of total energy as follows:

$$E = e + \frac{1}{2}u^2 + \frac{1}{2}v^2.$$

Finally, the mixture sound speed for isobaric closure has been calculated via:

$$c = \frac{\sum y_k \varepsilon_k c_k^2}{\varepsilon} \tag{3}$$

where, y_k is the mass fraction and it is given by $y_k = \alpha_k \rho_k / \rho$, c_k is the speed of sound of the kth fluid and $\varepsilon_k = 1/(\gamma_k - 1)$.

2.3 Quasi-Linear Equations of the Reduced Model

In two-dimensional flow with two fluids, the system of Eq. (1) can be re-written in quasi-linear form with primitive variables in the following compact form:

$$\frac{\partial W}{\partial t} + A\,(W)\,\frac{\partial W}{\partial x} + B\,(W)\,\frac{\partial W}{\partial y} = 0 \tag{4}$$

where the primitive vector W and the Jacobian matrices $A(W)$ and $B(W)$ for this system can be written as:

$$W = \begin{bmatrix} \alpha_1 \\ \rho_1 \\ \rho_2 \\ u \\ v \\ P \end{bmatrix}, \quad A(W) = \begin{bmatrix} u & 0 & 0 & 0 & 0 & 0 \\ 0 & u & 0 & \rho_1 & 0 & 0 \\ 0 & 0 & u & \rho_2 & 0 & 0 \\ 0 & 0 & 0 & u & 0 & 1/\rho \\ 0 & 0 & 0 & 0 & u & 0 \\ 0 & 0 & 0 & \rho c^2 & 0 & u \end{bmatrix}$$

and

$$B(W) = \begin{bmatrix} v & 0 & 0 & 0 & 0 & 0 \\ 0 & v & 0 & 0 & \rho_1 & 0 \\ 0 & 0 & v & 0 & \rho_2 & 0 \\ 0 & 0 & 0 & v & 0 & 0 \\ 0 & 0 & 0 & 0 & v & 1/\rho \\ 0 & 0 & 0 & 0 & \rho c^2 & v \end{bmatrix}.$$

The Jacobian matrix $A(W)$ provides the following eigenvalues: $u + c, u, u, u, u$ and $u - c$, whereas the Jacobian matrix $B(W)$ provides the following eigenvalues: $v + c, v, v, v, v$ and $v - c$, which represent the wave speeds of the system.

3 Numerical Method

The numerical algorithm for 2d problems is developed using an extended Godunov approach with the classical MUSCL scheme to achieve second order accuracy in space and time. The splitting scheme is applied for the discretization of the conservative vector in two time steps as follows:

$$U_{i,j}^{n+\frac{1}{2}} = U_{i,j}^{n} - \frac{\Delta t}{\Delta x}\left[F^n\left(U^*\left(U_{i+\frac{1}{2},j}^{-}, U_{i+\frac{1}{2},j}^{+}\right)\right) - F^n\left(U^*\left(U_{i-\frac{1}{2},j}^{-}, U_{i-\frac{1}{2},j}^{+}\right)\right)\right] \text{ and}$$

$$U_{i,j}^{n+1} = U_{i,j}^{n+\frac{1}{2}} - \frac{\Delta t}{\Delta y}\left[G^{n+\frac{1}{2}}\left(U^*\left(U_{i,j+\frac{1}{2}}^{-}, U_{i,j+\frac{1}{2}}^{+}\right)\right) - G^{n+\frac{1}{2}}\left(U^*\left(U_{i,j-\frac{1}{2}}^{-}, U_{i,j-\frac{1}{2}}^{+}\right)\right)\right].$$

The flux vectors in x–direction $F(U^*)$ and in $y-$direction $G(U^*)$ have been calculated using HLL Riemann solver, which was first presented in [17] and described in the context of the Riemann problem with details in [18].

Similarly, the discretization of the volume fraction equation with second order accuracy can be written as:

$$\alpha_{i,j}^{n+\frac{1}{2}} = \alpha_{i,j}^{n} - u\frac{\Delta t}{\Delta x}\left[\alpha^{*(n)}\left(\alpha_{i+\frac{1}{2},j}^{-}, \alpha_{i+\frac{1}{2},j}^{+}\right) - \alpha^{*(n)}\left(\alpha_{i-\frac{1}{2},j}^{-}, \alpha_{i-\frac{1}{2},j}^{+}\right)\right] \text{ and}$$

$$\alpha_{i,j}^{n+1} = \alpha_{i,j}^{n+\frac{1}{2}} - v\frac{\Delta t}{\Delta y}\left[\alpha^{*(n+\frac{1}{2})}\left(\alpha_{i,j+\frac{1}{2}}^{-}, \alpha_{i,j+\frac{1}{2}}^{+}\right) - \alpha^{*(n+\frac{1}{2})}\left(\alpha_{i,j-\frac{1}{2}}^{-}, \alpha_{i,j-\frac{1}{2}}^{+}\right)\right].$$

The numerical time step size Δt is chosen as in [18]:

$$\Delta t = CFL \times \min\left(\frac{\Delta x}{S_x}, \frac{\Delta y}{S_y}\right),$$

where CFL is the Courant-Friedrichs-Lewy number (CFL ≤ 1, to insure the stability of the numerical method), S_x and S_y are the maximum wave speeds in the x and y directions respectively and they can be expressed as:

$$S_x = \max(0, u^+_{i\pm\frac{1}{2},j} + c^+_{i\pm\frac{1}{2},j}, u^-_{i\pm\frac{1}{2},j} + c^-_{i\pm\frac{1}{2},j}),$$
$$S_y = \max(0, v^+_{i,j\pm\frac{1}{2}} + c^+_{i,j\pm\frac{1}{2}}, v^-_{i,j\pm\frac{1}{2}} + c^-_{i,j\pm\frac{1}{2}}).$$

3.1 2D Form of the HLL Approximate Riemann Solver

With HLL Riemann solver, the numerical flux function at a cell boundary in x–direction can be written as follows:

$$F^{HLL}_{i+\frac{1}{2},j} = \begin{cases} F_{i,j} & \text{if } 0 \leq S_{XL}, \\ \dfrac{S^+_{i+\frac{1}{2},j} F_{i,j} - S^-_{i+\frac{1}{2},j} F_{i+1,j} + S^+_{i+\frac{1}{2},j} S^-_{i+\frac{1}{2},j} (U_{i+1,j} - U_{i,j})}{S^+_{i+\frac{1}{2},j} - S^-_{i+\frac{1}{2},j}} & \text{if } S_{XL} \leq 0 \leq S_{XR}, \\ F_{i+1,j} & \text{if } 0 \geq S_{XR} \end{cases}$$

In the similar way the numerical flux function at a cell boundary in $y-$direction can be written as follows:

$$G^{HLL}_{i,j+\frac{1}{2}} = \begin{cases} G_{i,j} & \text{if } 0 \leq S_{YL}, \\ \dfrac{S^+_{i,j+\frac{1}{2}} G_{i,j} - S^-_{i,j+\frac{1}{2}} G_{i,j+1} + S^+_{i,j+\frac{1}{2}} S^-_{i,j+\frac{1}{2}} (U_{i,j+1} - U_{i,j})}{S^+_{i,j+\frac{1}{2}} - S^-_{i,j+\frac{1}{2}}} & \text{if } S_{YL} \leq 0 \leq S_{YR}, \\ G_{i,j+1} & \text{if } 0 \geq S_{YR} \end{cases}$$

where subscripts S_{XR} and S_{XL} denotes to right and left wave speeds at each cell boundary in $x-$direction . Whereas, S_{YR} and S_{YL} denotes to right and left wave speeds at each cell boundary in $y-$direction.

4 Test Problems

Four different test cases have been considered to observe the evolution of the interface and to assess the numerical algorithm that is developed in this work. These cases consider different initial states and physical properties, which provide different flow

Table 1 Initial conditions for the explosion test

Physical property	Bubble	Surrounding fluid
Density, kg/m^3	1	0.125
X-Velocity, m/s	0	0
Y- Velocity, m/s	0	0
Pressure, Pa	1	0.1
Heat capacity ratio, γ	1.4	1.4

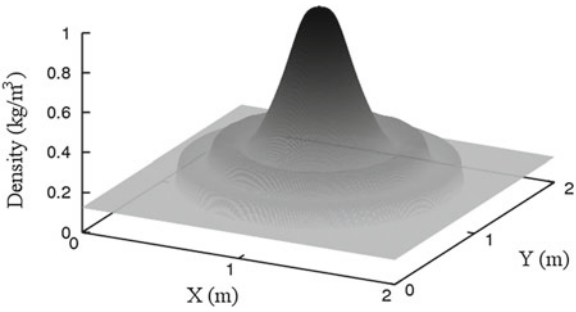

Fig. 1 Evolution of density profile at t = 0.25 s for the explosion test

regimes. The results obtained from the first three cases have been compared with other numerical results which are generated using different models and numerical methods. In the fourth case the current results have been compared with available experimental data.

4.1 Explosion Test

This test is a single phase problem and the reduced model of the two-phase flows is applied for this test. In this test the two flow components stand for the same fluid which produce extreme conditions. The physical domain of this problem is a square of 2×2 m, which contains a circular bubble of 0.8 m in diameter located at the center of the domain. The initial condition is demonstrated in Table 1. The computation was made using 300×300 cells and the periodic boundary conditions (B.C) were considered.

The surface plots for density and pressure distribution at time t = 0.25 s are illustrated in Figs. 1 and 2 respectively. The current results are significantly close to the results that published in [18]. This confirms that the reduced model reproduces the physical behavior of the flow components with stiff initial conditions.

4.2 Interface Translation Test

The computational domain for this case study is a square of 1×1 m includes a circular interface of 0.32 m in diameter separates two fluids. The center of the bubble

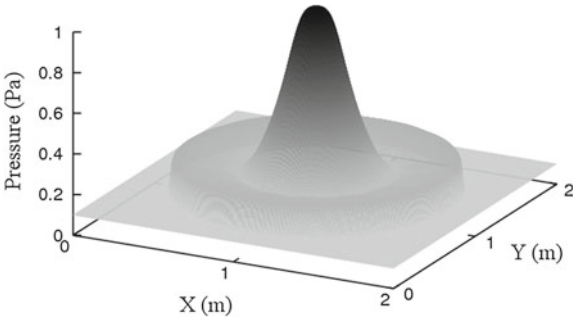

Fig. 2 Evolution of pressure profile at t = 0.25 s for the explosion test

Table 2 Initial conditions for the interface test

Physical property	Bubble	Surrounding fluid
Density, kg/m^3	1	0.1
X-Velocity, m/s	1	1
Y- Velocity, m/s	1	1
Pressure, Pa	1	1
Heat capacity ratio, γ	1.4	1.6

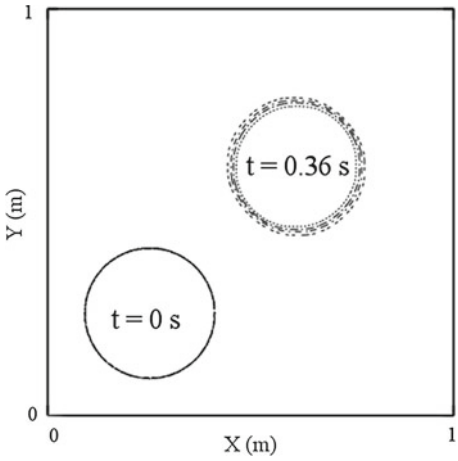

Fig. 3 Volume fraction contours at the initial time t = 0 s and at time t = 0.36 s for the interface translation test

is located at 0.25, 0.25 m. The initial conditions for this test are stated in Table 2. The computation was made using 300 × 300 cells and periodic B.C.

The results are shown in Fig. 3 for volume fraction contours at the initial time t = 0 s and at the time t = 0.36 s. The results show the time interval during which the bubble has moved with a uniform velocity and pressure from its initial position to a new location where the center of the bubble has the coordinates (0.61, 0.61) m. The shape of the bubble can be compared with the numerical results presented in [19].

Table 3 Initial conditions for the under-water explosion test

Physical property	Bubble	Surrounding fluid
Density, kg/m^3	1.241	0.991
X-Velocity, m/s	0	0
Y- Velocity, m/s	0	0
Pressure, Pa	2.753	3.059e^{-4}
Heat capacity ratio, γ	1.4	5.5
Pressure constant, π	0	1.505

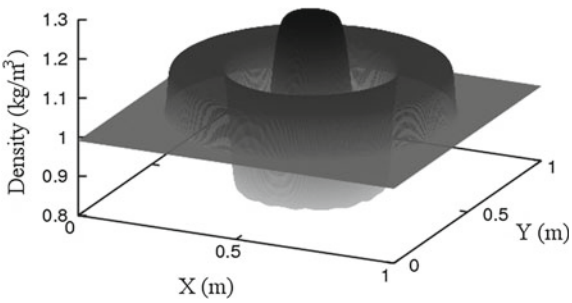

Fig. 4 Density evolution at time t = 0.058 s for the explosion under-water test

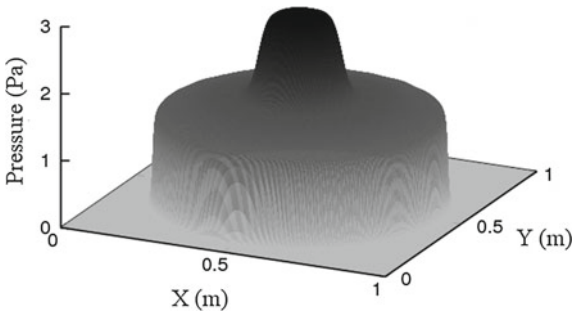

Fig. 5 Pressure distribution at time t = 0.058 s for the explosion under-water test

4.3 Bubble Explosion Under-Water Test

This test has been considered by many researchers, for example [15] and [19]. The computational domain of this test problem is a square of dimension 1×1 m, which including a bubble of 0.4 m in diameter located in the center of the domain. The initial state is shown in Table 3. The simulation was made using 300×300 cells and periodic B.C.

The surface plots for mixture density and pressure are presented in Figs. 4 and 5 respectively. The numerical results obtained are compared with the equivalent numerical results that published in [15] and [19]. The current results demonstrate a good compatibility with the other results. The numerical solutions obtained characterize and capture the physical behavior and the evolution of the interface correctly.

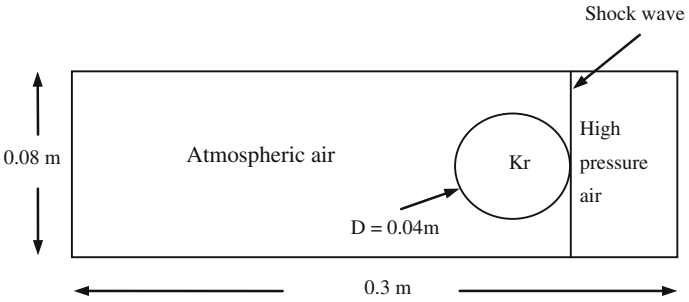

Fig. 6 Schematic diagram shows the physical domain of shock-bubble interaction test

Table 4 Initial conditions for shock-bubble interaction test

Physical property	Krypton bubble	Pre-shock air	Post-shock air
Density, kg/m^3	3.506	1.29	2.4021
X-Velocity, m/s	0	0	230.28
Y- Velocity, m/s	0	0	0
Pressure, Pa	101325	101325	249091
Heat capacity ratio, γ	1.67	1.4	1.4

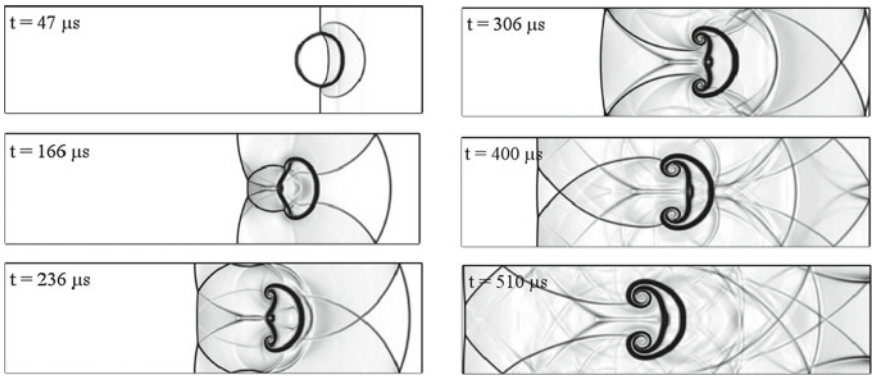

Fig. 7 The mixture density contours for the krypton bubble-air constitution at different times t = 47μs, 166 μs, 236 μs, 306 μs, 400 μs and 510 μs

4.4 Validation of Shock-Bubble Interaction

Here the interaction between a moderate shock wave (Mach = 1.5) and Krypton gas bubble surrounded by air at atmospheric pressure has been simulated. The current numerical results have been compared with the experimental results in [11]. A schematic diagram of the initial physical state is illustrated in Fig. 6 and the initial conditions are shown in Table 4.

The results are demonstrated in Fig. 7. The evolution of the bubble contour with time due to the interaction with the shock wave is observable and it is in a good agreement with experimental results in [11]. It can be noticed that the present numerical method has the mechanism for tracking the physical phenomena that have been occurrence within the domain of the interaction. At the early stage of the interaction, one can notice a shock wave transmitting inside the gas bubble, incident shock outside the bubble and a reflection wave propagating backward to the right side. The deformation of the bubble is influenced by the differences in densities between the krypton and surrounded air especially in the early stages of the interaction. In the middle time a high speed penetrating jet, which moving towards the right side has generated on the line of symmetry of the bubble. At relatively later stages the effect of the vorticity on the interface deformation has appeared. One can observe the vortices that have been generated on the top and at the bottom of the bubble contour.

5 Conclusion

Numerical simulations of compressible flows between two immiscible fluids have been performed successfully. The numerical algorithm for these simulations has been developed based on an extended Godunov approach with HLL solver considering second order accuracy. The performance of the considered multi-component flow model and the numerical method has been verified effectively. This has been made using a set of carefully chosen case studies which are distinguished by a variety of compressible flow regimes. The obtained results show that the developed algorithm is able to reproduce the physical behavior of the flow components efficiently. Consequently, it could be applied to simulate a wide range of compressible multi-component flows with different materials and physical properties.

References

1. Lindl JD, McCrory RL, Campbell EM (1992) Progress toward ignition and burn propagation in inertial confinement fusion. Phys Today 45(9):32–40
2. Nowakowski A, Librovich B, Lue L (2004) Reactor safety analysis based on a developed two-phase compressible flow simulation. In: Proceedings of the 7th Biennial conference on engineering systems design and analysis, ESDA 2004, Manchester, U.K, 19–22 July 2004, vol 1, pp 929–936
3. Saurel R, Abgrall R (1999) A multiphase Godunov method for compressible multifluid and multiphase flows. J Comput Phys 150(2):425–467
4. Allaire G, Clerc S, Kokh S (2000) A five-equation model for the numerical simulation of interfaces in two-phase flows, C. R. Acad Sci—Series I: Mathematics 331(12):1017–1022
5. Murrone A, Guillard H (2005) A five-equation model for the simulation of interfaces between compressible fluids. J Comput Phys 202(2):664–698

6. Kapila AK, Menikoff R, Bdzil JB, Son SF, Stewart DS (2001) Two-phase modeling of deflagration to detonation transition in granular materials: reduced equations. Phys Fluids 13(10):3002–3024
7. Allaire G, Clerc S, Kokh S (2002) A five-equation model for the simulation of interfaces between compressible fluids. J Comput Phys 181(2):577–616
8. Ballil A, Jolgam S, Nowakowski AF, Nicoleau FCGA (2012) Numerical simulation of compressible two-phase flows using an Eulerian type reduced model. In: Proceedings of the world congress on engineering WCE 2012. Lecture Notes in Engineering and Computer Science. U.K, London, 4–6 July 2012, pp 1835–1840
9. Haas JF, Sturtevant B (1987) Interaction of weak shock waves with cylindrical and spherical gas inhomogeneities. J Fluid Mech 181:41–76
10. Layes G, Jourdan G, Houas L (2003) Distortion of a spherical gaseous interface accelerated by a plane shock wave. Phys Rev Lett 91(17):174502
11. Layes G, Le Métayer O (2007) Quantitative numerical and experimental studies of the shock accelerated heterogeneous bubbles motion. Phys Fluids 19:042105
12. Coquel F, Amine KE, Godlewski E, Perthame B, Rascle P (1997) A numerical method using upwind schemes for the resolution of two-phase flows. J Comput Phys 136:272–288
13. Bagabir A, Drikakis D (2001) Mach number effects on shock-bubble interaction. Shock Waves 11(3):209–218
14. Hu X, Khoo B (2004) An interface interaction method for compressible multifluids. J Comput Phys 198:35–64
15. Terashima H, Tryggvason G (2010) A front-tracking method with projected interface conditions for compressible multi-fluid flows. Comput Fluids 39:1804–1814
16. Shukla RK, Pantano C, Freund JB (2010) An interface capturing method for the simulation of multi-phase compressible flows. J Comput Phys 229:7411–7439
17. Harten A, Lax PD, Leer BV (1983) On upstream di_erencing and Godunov-type schemes for hyperbolic conservation laws. SIAM Review 25(1):35–61
18. Toro E (1999) Riemann solvers and numerical methods for fluid dynamics. Springer
19. Shyue K (1998) An efficient shock-capturing algorithm for compressible multi-component problems. J Comput Phys 142(1):208–242